Title

Reductions in brain pericytes are associated with arteriovenous malformation vascular instability.

Journal

Journal of neurosurgery, 129(6)

ISSN

0022-3085

Authors

Winkler, Ethan A
Birk, Harjus
Burkhardt, Jan-Karl
et al.

Publication Date

2018-12-01

DOI

10.3171/2017.6.jns17860

Peer reviewed

Published in final edited form as:

J Neurosurg. 2018 December 01; 129(6): 1464–1474. doi:10.3171/2017.6.JNS17860.

Reductions in brain pericytes are associated with arteriovenous malformation vascular instability

Ethan A. Winkler, MD, PhD[1,2], **Harjus Birk, MD**[1], **Jan-Karl Burkhardt, MD**[1], **Xiaolin Chen, MD**[2,3], **John K. Yue, BS**[1], **Diana Guo, BA**[2], **W. Caleb Rutledge, MD**[1,2], **George F. Lasker, MD, PhD**[1], **Carlene Partow, BS**[1], **Tarik Tihan, MD, PhD**[4], **Edward F. Chang, MD**[1], **Hua Su, MD**[2], **Helen Kim, PhD**[2], **Brian P. Walcott, MD**[1,2,5], and **Michael T. Lawton, MD**[1,2]

[1]Department of Neurological Surgery, University of California, San Francisco

[2]Center for Cerebrovascular Research, Department of Anesthesia and Perioperative Care, University of California, San Francisco

[3]Department of Neurological Surgery, Beijing Tiantan Hospital, Capital Medical University, Beijing, People's Republic of China

[4]Department of Pathology, University of California, San Francisco

[5]Department of Neurological Surgery, University of Southern California, Los Angeles, California

Abstract

OBJECTIVE—Brain arteriovenous malformations (bAVMs) are rupture-prone tangles of blood vessels with direct shunting of blood flow between arterial and venous circulations. The molecular and/or cellular mechanisms contributing to bAVM pathogenesis and/or destabilization in sporadic lesions have remained elusive. Initial insights into AVM formation have been gained through models of genetic AVM syndromes. And while many studies have focused on endothelial cells, the contributions of other vascular cell types have yet to be systematically studied. Pericytes are multifunctional mural cells that regulate brain angiogenesis, blood-brain barrier integrity, and vascular stability. Here, the authors analyze the abundance of brain pericytes and their association with vascular changes in sporadic human AVMs.

METHODS—Tissues from bAVMs and from temporal lobe specimens from patients with medically intractable epilepsy (nonvascular lesion controls [NVLCs]) were resected. Immunofluorescent staining with confocal microscopy was performed to quantify pericytes (platelet-derived growth factor receptor–beta [PDGFRβ] and aminopeptidase N [CD13]) and extravascular hemoglobin. Iron-positive hemosiderin deposits were quantified with Prussian blue

Correspondence: Michael T. Lawton: Barrow Neurological Institute, Phoenix, AZ. michael.lawton@barrowbrainandspine.com.

Disclosures

The authors report no conflict of interest concerning the materials or methods used in this study or the findings specified in this paper.

Author Contributions

Conception and design: Lawton, Winkler, Tihan, Su, Kim, Walcott. Acquisition of data: Winkler, Birk, Burkhardt, Chen, Guo, Rutledge, Lasker, Partow, Tihan, Chang. Analysis and interpretation of data: Winkler, Birk, Burkhardt, Su, Kim, Walcott. Drafting the article: Winkler, Burkhardt, Chen, Yue, Lasker. Critically revising the article: Lawton, Winkler, Rutledge, Su, Kim, Walcott. Reviewed submitted version of manuscript: Lawton, Winkler, Su, Kim, Walcott. Approved the final version of the manuscript on behalf of all authors: Lawton. Statistical analysis: Winkler, Yue. Study supervision: Lawton.

staining. Syngo iFlow post–image processing was used to measure nidal blood flow on preintervention angiograms.

RESULTS—Quantitative immunofluorescent analysis demonstrated a 68% reduction in the vascular pericyte number in bAVMs compared with the number in NVLCs ($p < 0.01$). Additional analysis demonstrated 52% and 50% reductions in the vascular surface area covered by CD13- and PDGFRβ-positive pericyte cell processes, respectively, in bAVMs ($p < 0.01$). Reductions in pericyte coverage were statistically significantly greater in bAVMs with prior rupture ($p < 0.05$). Unruptured bAVMs had increased microhemorrhage, as evidenced by a 15.5-fold increase in extravascular hemoglobin compared with levels in NVLCs ($p < 0.01$). Within unruptured bAVM specimens, extravascular hemoglobin correlated negatively with pericyte coverage (CD13: $r = -0.93$, $p < 0.01$; PDGFRβ: $r = -0.87$, $p < 0.01$). A similar negative correlation was observed with pericyte coverage and Prussian blue–positive hemosiderin deposits (CD13: $r = -0.90$, $p < 0.01$; PDGFRβ: $r = -0.86$, $p < 0.01$). Pericyte coverage positively correlated with the mean transit time of blood flow or the time that circulating blood spends within the bAVM nidus (CD13: $r = 0.60$, $p < 0.05$; PDGFRβ: $r = 0.63$, $p < 0.05$). A greater reduction in pericyte coverage is therefore associated with a reduced mean transit time or faster rate of blood flow through the bAVM nidus. No correlations were observed with time to peak flow within feeding arteries or draining veins.

CONCLUSIONS—Brain pericyte number and coverage are reduced in sporadic bAVMs and are lowest in cases with prior rupture. In unruptured bAVMs, pericyte reductions correlate with the severity of microhemorrhage. A loss of pericytes also correlates with a faster rate of blood flow through the bAVM nidus. This suggests that pericytes are associated with and may contribute to vascular fragility and hemodynamic changes in bAVMs. Future studies in animal models are needed to better characterize the role of pericytes in AVM pathogenesis.

Keywords

pericytes; arteriovenous malformations; blood-brain barrier; microhemorrhage; intracerebral hemorrhage; stroke; vascular disorders

Brain arteriovenous malformations (bAVMs) are rupture-prone tangles of blood vessels with direct shunting of blood flow between arterial and venous circulations without a clear intervening capillary bed.[18,26,43] Rates of intracerebral hemorrhage range from 1% to 3% per person-year, often with catastrophic neurological consequences.[11] Numerous structural abnormalities suggestive of instability have been described, including dilated perinidal capillary networks,[4,28,34] intranidal or feeding artery aneuryms,[11] and/or microhemorrhage.[1,12,24] However, the cellular and/or molecular mechanisms underlying bAVM destabilization or rupture have remained elusive.

Normal cerebrovascular structure and function depend on the coordinated signaling of multiple interconnected cell types, including endothelial cells, mural cells (vascular smooth muscle cells and pericytes), immune cells, glia, and neurons.[8,34] Pericytes are the principal mural cell population of the cerebral microvasculature, covering roughly 80%–90% of the vascular wall.[6,38,40] Pericytes fulfill a modulatory role in a number of integral cerebrovascular functionalities, which are disrupted in bAVMs, including regulation of brain angiogenesis, endothelial proliferation, vascular diameter, blood flow regulation, vascular

wall stability, and integrity of the blood-brain barrier (BBB).[2,31,44] Qualitative studies have suggested that pericytes may be reduced in human bAVMs and/or rodent models of bAVM.[8,34] However, pericytes have yet to be systematically studied, and many published reports have focused exclusively on the endothelium.

In the present study, we quantified pericyte abundance in resected sporadic human bAVMs and studied their association with vascular changes. We report not only that pericytes are reduced in bAVMs, but also that the reductions are associated with indices of instability, for example, clinically significant rupture and microhemorrhage, and alterations in nidal blood flow.

Methods

Human Subjects

Tissue specimens were obtained from bAVMs that had been resected by the senior author (M.T.L.). For nonvascular lesion controls (NVLCs), temporal lobe specimens were similarly acquired from subjects undergoing anterior temporal lobectomy for medically refractory epilepsy (E.F.C.). All tissues were immersion fixed in formaldehyde and embedded in paraffin blocks for neuropathological analysis. In total, 30 bAVM tissue specimens were obtained from neuropathology, but 10 samples were either too small or of too poor quality to be included in our analysis. There were 11 control samples. A summary of subject characteristics is provided in Table 1. This study was approved by the University of California, San Francisco, Institutional Review Board and performed in compliance with the Health Insurance Portability and Accountability Act regulations.

Immunofluorescent Analysis

Brain pericyte and hemoglobin immunodetection was performed as previously described.[6,30,39,40] Embedded tissue specimens were sectioned using a microtome at a thickness of 6 μm. Sections were then deparaffinized and rehydrated with serial ethanol washes to distilled water. All sections were boiled in target antigen retrieval solution, pH 9 (Dako), for 20 minutes in a conventional microwave. Following antigen retrieval, tissue sections were blocked in 10% normal swine serum (Vector Laboratories) with 0.05% Triton X-100 (Sigma-Aldrich) for 1 hour at room temperature. Sections were then incubated with the following primary antibodies at 4°C: goat anti–human platelet-derived growth factor receptor–beta (PDGFRβ; 1:100, R&D Systems), mouse anti–human aminopeptidase N (CD13; 1:100, R&D Systems), goat antihemoglobin (10 μg/ml, R&D Systems), mouse anti–human glial fibrillary acidic protein (GFAP; Cell Signaling Inc.), and/or rabbit anti–human platelet endothelial adhesion molecule 1 (CD31; 1:25, Abcam Inc.). Sections were then washed in phosphate-buffered saline containing 0.05% Triton X-100 and incubated in secondary antibody for 1 hour at room temperature. To visualize pericytes, sections were incubated in bovine anti–goat Cy3 (Jackson ImmunoResearch Laboratories Inc.) and donkey anti–mouse Alexa Fluor 488 (Jackson Laboratories) antibodies to detect PDGFRβ and CD13, respectively. To visualize astrocytes, sections were incubated with donkey anti–mouse Alexa Fluor 488 (Jackson Laboratories) antibodies to detect GFAP. To visualize extravascular hemoglobin, sections were incubated in bovine anti–goat Cy3 antibody

(Jackson Laboratories). To visualize endothelium, sections were incubated in biotinylated horse anti–rabbit antibody (Jackson Laboratories) or biotinylated *Ulex europaeus* agglutinin 1 (lectin, Vector Laboratories), followed by incubation in DyLight 649–conjugated streptavidin (Vector Laboratories). All sections were incubated in 1% Sudan Black B diluted in 70% ethanol for 10 minutes at room temperature to quench autofluorescence.

Following completion of immunodetection, tissue sections were mounted with fluorescent mounting medium (Dako) and coverslipped. All imaging was performed with a Leica TCS SP5 X confocal microscope utilizing a 20× objective (Leica Microsystems Inc.). For all imaging, identical laser settings were used for AVMs and NVLCs. Representative images were prepared with NIH ImageJ software.

Image Analysis

All analyses were performed with NIH ImageJ software. Ten- to 12-μm maximum projection z-stack images were reconstructed. For all studies, 3–5 randomly selected fields in 3 nonadjacent tissue sections per tissue specimen were analyzed as previously described.[30,39] For pericyte coverage analysis, PDGFRβ- or CD13-positive surface area was measured with the ImageJ Area measurement tool and divided by the CD31-positive endothelial surface area as previously described.[6,30,38,40] For pericyte number analysis, pericyte cell bodies were manually counted and divided by the CD31-positive endothelial surface area as previously described.[6,30,38,40] Extravascular hemoglobin was quantified as previously described.[39,40] The intravascular hemoglobin-positive immunofluorescent signal was subtracted from maximum projection z-stack images utilizing the ImageJ colocalization function as previously described.[40] The remaining extravascular hemoglobin-positive immunofluorescent signal was subjected to threshold processing and quantified with ImageJ Integrated Density analysis. Variability in background staining was minimized with post–image thresholding. All image analyses were performed by an investigator blinded to the pathological diagnosis to avoid the introduction of bias.

Hemosiderin Deposits

Formaldehyde-fixed paraffin-embedded tissue sections were deparaffinized and rehydrated. Prussian blue staining was then performed as described by the manufacturer utilizing an iron staining kit (Abcam Inc.). Nuclear fast red was used as a counterstain. Sections were subsequently coverslipped using Shandon-Mount mounting medium (Thermo Scientific) and imaged with a Leica DMI6000 inverted epifluorescence microscope (Leica Microsystems Inc.). Prussian blue hemosiderin deposits were manually counted by a blinded investigator and expressed per square millimeter of tissue.

AVM Blood Flow Analysis

Syngo iFlow post–image processing software (Siemens) was used to reconstruct color-coded preoperative digital subtraction angiograms (Axiom Artis, Siemens) when available. The syngo iFlow software condenses the complete digital subtraction angiography run into a single color-coded image to facilitate quantification of hemodynamic parameters. A region of interest (ROI) was manually drawn over the caliber of selected vessels. A time versus intensity graph was generated, which permitted quantification of the ROI peak time (Tmax)

—this is defined as the time to peak contrast intensity in the selected vascular ROI. Nidal mean transit time (MTT) was next figured by calculating the difference between the Tmax of the closest arterial feeding artery and venous outflow in the draining vein. In the instance of multiple feeding arteries and/or draining veins, the fastest MTT of the nidus was selected for each subject. The MTT is a measure of the time that circulating blood spends within the bAVM nidus; therefore, a higher MTT suggests a slower rate of flow, whereas a lower MTT suggests a faster rate of blood flow.

Statistical Analysis

All continuous variables were analyzed with the Student t-test to determine differences between AVMs and NVLCs. For categorical variables, either a Fisher's exact test or chi-square test was performed to analyze differences between groups. Pearson's correlation coefficient (r) was used for all correlations. A p value < 0.05 was considered the threshold for statistical significance in all analyses. Values are presented as the mean ± standard error of the mean unless otherwise specified.

Results

Pericytes Reduced in Human bAVMs

Pericytes are perivascular cells embedded in a common vascular basement membrane on the abluminal endothelial cell membrane and comprise both a cell body and stellate-shaped finger-like cell processes, which ensheathe the endothelial vascular tube (Fig. 1). Using established methodologies, we quantified both pericyte number and coverage. In total, reductions in vascular pericytes as measured by both parameters were observed in all 20 bAVM specimens. Quantitative analysis demonstrated a statistically significant 68% reduction in the CD13-positive pericyte number in bAVMs compared with the number in NVLCs (bAVMs 862.2 ± 47.3 pericytes per mm^2 vascular surface area; NVLCs 2657.0 ± 140.7 pericytes per mm^2 vascular surface area; $p < 0.01$; Fig. 2A and B). Similar analysis utilizing the independent pericyte cell marker PDGFRβ confirmed a statistically significant 68% reduction in the pericyte cell number between bAVMs and NVLCs (bAVMs 845.6 ± 47.9 pericytes per mm^2 vascular surface area; NVLCs 2658.1 ± 174.8 pericytes per mm^2 vascular surface area; $p < 0.01$; Fig. 2C).

We next quantified pericyte cell coverage of the cerebrovascular wall, which is the percentage of the vascular wall covered by pericyte cell processes. Quantitative immunofluorescent analysis demonstrated a statistically significant 52.3% reduction in the vascular surface area covered by CD13-positive pericyte cell processes (bAVMs 39.4% ± 2.8%; NVLCs 82.7% ± 2.1%; $p < 0.01$; Fig. 2D). These analyses were confirmed utilizing the independent pericyte cell marker PDGFRβ, which demonstrated a similar statistically significant 49.9% reduction in PDGFRβ-positive pericyte cell coverage between bAVMs and NV-LCs (bAVMs 40.6% ± 2.5%; NVLCs 81.3% ± 2.3%; $p < 0.01$; Fig. 2E). These data suggest that both pericyte cell number and coverage of the vascular wall are reduced in sporadic human bAVMs.

Magnitude of Pericyte Reductions in Ruptured bAVMs

Having demonstrated a reduction in pericyte number and coverage in bAVMs, we used similar analyses to determine whether differences in pericyte populations existed between ruptured and unruptured bAVMs. No statistically significant difference in the CD13- and PDGFRβ-positive pericyte cell number was demonstrated between unruptured and ruptured bAVM cohorts (Table 2). However, quantitative immunofluorescent analysis of the vascular coverage of CD13- and PDGFRβ-positive cell processes showed 25.7% and 20.7% greater reductions in pericyte coverage, respectively, in ruptured than in unruptured bAVMs. These data suggest that pericyte coverage, but not pericyte number, is further reduced in bAVMs with clinically significant rupture.

Reductions in Pericyte Populations in Unruptured bAVMs

Silent microhemorrhage has been proposed as a risk factor for future bAVM rupture and may serve as a surrogate for the relative instability of a subset of bAVMs.[1,12] Therefore, we investigated whether the observed reductions in pericytes correlated with the extent of acute and chronic microhemorrhage in the unruptured bAVM group. Quantitative immunofluorescent analysis demonstrated a statistically significant 15.5-fold increase in extravascular hemoglobin consistent with acute microhemorrhage in unruptured bAVMs compared with that in NVLCs (mean extravascular hemoglobin integrated density: bAVMs 1,206,583 ± 307,333 units; NVLCs 77,742.4 ± 30,829 units; $p < 0.01$; Fig. 3A and B). Within the unruptured bAVMs, pericyte coverage correlated negatively with the extent of microhemorrhage (CD13-positive pericyte coverage: $r = -0.93$, $p < 0.01$; PDGFRβ-positive pericyte coverage: $r = -0.87$, $p < 0.01$; Fig. 3C and D). This suggests that lower pericyte coverage is associated with greater microhemorrhage within unruptured bAVMs.

To confirm these results, we investigated whether a similar relationship was present between pericyte coverage and chronic microhemorrhage as evidence by Prussian blue–positive hemosiderin deposits. This analysis demonstrated a statistically significant 21.5-fold increase in perivascular hemosiderin deposits in unruptured bAVMs compared with those in NVLCs (bAVMs 0.46 ± 0.11 deposits; NVLCs 0.02 ± 0.01 deposits; $p < 0.01$; Fig. 4A and B). As observed with acute microhemorrhage, pericyte coverage correlated negatively with Prussian blue–positive hemosiderin deposits in unruptured bAVMs (CD13-positive pericyte coverage: $r = -0.90$, $p < 0.01$; PDGFRβ-positive pericyte coverage: $r = -0.86$, $p < 0.01$; Fig. 4C and D). Collectively, these data suggest that lower pericyte coverage is associated with greater microhemorrhage in unruptured bAVMs.

bAVM Pericyte Reductions and Nidal Blood Flow

In addition to stabilizing the cerebrovasculature, pericytes contribute to the regulation of regional cerebral blood flow.[6,13,17,22] Therefore, we used syngo iFlow technology on preintervention angiograms when available to quantify blood flow through the bAVM nidus to determine whether reductions in bAVM pericyte populations are associated with alterations in nidal blood flow. Within bAVMs with compatible preoperative angiograms (12 cases), pericyte coverage correlated positively with the MTT of injected contrast through the nidus (CD13-positive pericyte coverage: $r = 0.60$, $p < 0.05$; PDGFRβ-positive pericyte coverage: $r = 0.63$, $p < 0.05$; Fig. 5). This suggests that greater pericyte coverage is

associated with a longer transit time or slow rates of blood flow through the bAVM nidus. Conversely, bAVMs with the greatest loss of pericytes demonstrated shorter transit times or faster rates of nidal blood flow. No statistically significant correlations were observed with time to peak flow within bAVM feeding arteries or draining veins (data not shown).

Discussion

In the present report, we demonstrate that a reduction in pericytes is associated with both vascular instability and altered hemodynamics in human bAVMs. Prior qualitative works have suggested that mural cells may be reduced in human bAVMs and/or rodent models of bAVM.[8,34] However, using 2 independent and established pericyte markers—CD13 and PDGFRβ—we provide the first quantitative evidence of a significant reduction in both pericyte cell number and coverage in human sporadic bAVMs. Consistent with prior reports on other pathologies, the magnitude of deficiency in the pericyte cell number exceeds what is observed with cell coverage.[6,30,40] Numerous reports have demonstrated that reductions in pericyte cell coverage are of greatest biological consequence and best correlate with indices of pericyte cell function.[3,6,9] This suggests in part that the remaining pericytes may hypertrophy and/or branch additional processes as a mechanism of potential compensation.

Pericytes exert a multitude of stabilizing effects on the cerebrovascular wall in vivo, including induction and maintenance of endothelial tight junctional protein complexes, deposition of perivascular extracellular matrix proteins, and inhibition of degradative enzymes, for example, matrix metalloproteinases.[3,6,7,9,35,38] Genetic depletion of brain pericytes in rodents results in cerebral vessels that display focal and/or diffuse dilations with increased tortuosity, which are prone to rupture and chronically leak circulating blood-derived plasma proteins.[3,6,10,16,20,21,35,36] In rodent bAVM models with deficient transforming growth factor–β (TGF-β) signaling through genetic depletion of vascular activin receptor-like kinase 1 (*Alk1*), a reduction in brain pericytes was correlated with leakage of circulating blood-derived fibrin, suggesting a compromised BBB.[8] However, the consequences of pericyte deficiency in human bAVMs are presently unknown.

To begin to elucidate the role of pericyte deficiency in human bAVMs, we adopted a correlative approach to define hypothesis-driven associations with known pericyte functions. Consistent with a potential stabilizing role of pericytes, reductions in pericyte coverage were greatest in bAVMs with prior rupture resulting in intracerebral hemorrhage. In unruptured bAVMs, clinically silent microhemorrhage portends a higher risk of future rupture and may represent a transitional state in the continuum of destabilization.[1,12,24] We showed that pericyte coverage reductions negatively correlate with acute and chronic microhemorrhages in unruptured human bAVMs. Although associative in nature, these data suggest that a greater loss of pericytes may contribute to a greater microhemorrhage burden and/or likelihood of rupture. However, the threshold of pericyte loss required to evoke vascular destabilization in bAVMs and/or other disease entities has yet to be elucidated.

In addition to stabilizing the vasculature, pericytes help to regulate resting cerebral blood flow and blood flow responses to neuronal activation—a concept known as “neurovascular coupling.”[6,13,17,22] Pericytes express contractile proteins and have been shown to modulate

vascular diameter both at rest and in response to a myriad of molecular cues.[3,13,25,41,42] In rodent models of bAVM, in vivo time-lapse multiphoton microscopy has demonstrated that progressive dilation of capillary beds contributes to arteriovenous shunting.[23] When quantitative iFlow analysis was applied to preintervention angiograms, we found that pericyte coverage positively correlates with the MTT of blood flow through the nidus in human bAVMs. This means that a greater reduction in pericyte coverage is associated with a reduced MTT, or a faster rate of flow, through the bAVM nidus. Pericyte deficiency has been associated with increases in vascular diameter and/or loss of vasomotor tone in vivo.[3,16,17] Whether this finding in human bAVMs is the result of changes in vascular diameter and/or vascular tone remains to be determined. Similarly, the ramifications of these hemodynamic changes on lesion stability and/or remodeling require future study.

It should be noted that pericyte deficiency is not unique to human bAVMs and has been previously reported in a number of human neurological diseases with vascular pathology, including Alzheimer's disease,[14,27,30] amyotrophic lateral sclerosis,[39,40] cavernous malformations,[29,33] and prenatal intraventricular hemorrhage.[5,20] Pericyte deficiency may therefore represent a common downstream pathway of vascular destabilization in the central nervous system. During brain angiogenesis, the recruitment of pericytes to nascent endothelial cell tubes relies on a complex interplay of multiple signal transduction cascades, including platelet-derived growth factor B (PDGF-B), TGF-β, Notch, vascular endothelial growth factor, and angiopoietin cell signaling.[2,31,35] Previously, PDGF-B levels were reported to be undetectable in a majority of bAVMs.[15] However, the inciting molecular event(s) for pericyte reductions in human bAVMs and whether it is unique among disease states with pericyte deficiency remain to be determined. In other disease states, such as hereditary hemorrhagic telangiectasia, pericytes can be therapeutically manipulated to stabilize the vascular wall and reduce bleeding.[19,32] Future studies are needed to evaluate the therapeutic potential of manipulating pericytes or, more broadly, mural cells in bAVMs.

This study was not without limitations, and the results should be appropriately framed. Experiments were conducted on resected bAVMs and may therefore reflect a selection bias toward more aggressive lesions that were clinically detected. Comparisons were also made utilizing an NVLC of resected temporal lobe from patients with medically refractory temporal lobe epilepsy and not from brain completely devoid of pathology. Prior reports have demonstrated that pericyte populations do not vary significantly within brain regions, and reported values for controls are in good agreement with previously reported values from postmortem nonepileptic human brain samples from multiple brain regions.[30,37,38] Nonetheless, the contribution of regional variability in pericyte abundance to the observed findings cannot be completely excluded. Finally, all relationships are associative and correlative in nature and do not imply causality. Future studies in rodent models are needed to more clearly delineate a causal relationship between pericyte loss and vascular changes in bAVMs.

Conclusions

Brain pericyte number and coverage are reduced in sporadic human bAVMs. Pericyte reductions are greatest in bAVMs with clinically significant hemorrhage and are associated

with a greater microhemorrhage burden in unruptured cases. Pericyte reduction also correlates with faster blood flow through the bAVM nidus. This suggests that pericytes are associated with and may contribute to vascular fragility and hemodynamic changes in human bAVMs. Future studies with animal models are needed to better characterize the role of pericytes in AVM pathogenesis and to determine whether these cells can be therapeutically targeted to promote bAVM stabilization.

Acknowledgments

This work was supported by the following grants: NIH grant no. RO1 NS034949 (H.K.); NIH grant nos. R01-NS027713 and R01-HL122774 and Michael Ryan Zodda Foundation (H.S.); National Natural Science Foundation of China 81500995 (X.C.); and Congress of Neurological Surgeons Christopher C. Getch Fellowship (B.P.W.).

ABBREVIATIONS

bAVM	brain arteriovenous malformation
BBB	blood-brain barrier
CD13	aminopeptidase N
CD31	platelet endothelial adhesion molecule 1
GFAP	glial fibrillary acidic protein
MTT	mean transit time
NVLC	nonvascular lesion control
PDGFRβ	platelet-derived growth factor receptor–beta
ROI	region of interest

References

1. Abla AA, Nelson J, Kim H, Hess CP, Tihan T, Lawton MT. Silent arteriovenous malformation hemorrhage and the recognition of “unruptured” arteriovenous malformation patients who benefit from surgical intervention. Neurosurgery. 76:592–600.2015; [PubMed: 25714514]
2. Armulik A, Genové G, Betsholtz C. Pericytes: developmental, physiological, and pathological perspectives, problems, and promises. Dev Cell. 21:193–215.2011; [PubMed: 21839917]
3. Armulik A, Genové G, Mäe M, Nisancioglu MH, Wallgard E, Niaudet C, et al. Pericytes regulate the blood-brain barrier. Nature. 468:557–561.2010; [PubMed: 20944627]
4. Attia W, Tada T, Hongo K, Nagashima H, Takemae T, Tanaka Y, et al. Microvascular pathological features of immediate perinidal parenchyma in cerebral arteriovenous malformations: giant bed capillaries. J Neurosurg. 98:823–827.2003; [PubMed: 12691408]
5. Ballabh P, Braun A, Nedergaard M. The blood-brain barrier: an overview: structure, regulation, and clinical implications. Neurobiol Dis. 16:1–13.2004; [PubMed: 15207256]
6. Bell RD, Winkler EA, Sagare AP, Singh I, LaRue B, Deane R, et al. Pericytes control key neurovascular functions and neuronal phenotype in the adult brain and during brain aging. Neuron. 68:409–427.2010; [PubMed: 21040844]
7. Bell RD, Winkler EA, Singh I, Sagare AP, Deane R, Wu Z, et al. Apolipoprotein E controls cerebrovascular integrity via cyclophilin A. Nature. 485:512–516.2012; [PubMed: 22622580]

8. Chen W, Guo Y, Walker EJ, Shen F, Jun K, Oh SP, et al. Reduced mural cell coverage and impaired vessel integrity after angiogenic stimulation in the Alk1-deficient brain. Arterioscler Thromb Vasc Biol. 33:305–310.2013; [PubMed: 23241407]
9. Daneman R, Zhou L, Kebede AA, Barres BA. Pericytes are required for blood-brain barrier integrity during embryogenesis. Nature. 468:562–566.2010; [PubMed: 20944625]
10. Enge M, Bjarnegård M, Gerhardt H, Gustafsson E, Kalén M, Asker N, et al. Endothelium-specific platelet-derived growth factor-B ablation mimics diabetic retinopathy. EMBO J. 21:4307–4316.2002; [PubMed: 12169633]
11. Gross BA, Du R. Natural history of cerebral arteriovenous malformations: a meta-analysis. J Neurosurg. 118:437–443.2013; [PubMed: 23198804]
12. Guo Y, Saunders T, Su H, Kim H, Akkoc D, Saloner DA, et al. Silent intralesional microhemorrhage as a risk factor for brain arteriovenous malformation rupture. Stroke. 43:1240–1246.2012; [PubMed: 22308253]
13. Hall CN, Reynell C, Gesslein B, Hamilton NB, Mishra A, Sutherland BA, et al. Capillary pericytes regulate cerebral blood flow in health and disease. Nature. 508:55–60.2014; [PubMed: 24670647]
14. Halliday MR, Rege SV, Ma Q, Zhao Z, Miller CA, Winkler EA, et al. Accelerated pericyte degeneration and blood-brain barrier breakdown in apolipoprotein E4 carriers with Alzheimer's disease. J Cereb Blood Flow Metab. 36:216–227.2016; [PubMed: 25757756]
15. Hashimoto T, Wu Y, Lawton MT, Yang GY, Barbaro NM, Young WL. Coexpression of angiogenic factors in brain arteriovenous malformations. Neurosurgery. 56:1058–1065.2005; [PubMed: 15854255]
16. Hellström M, Gerhardt H, Kalén M, Li X, Eriksson U, Wolburg H, et al. Lack of pericytes leads to endothelial hyperplasia and abnormal vascular morphogenesis. J Cell Biol. 153:543–553.2001; [PubMed: 11331305]
17. Kisler K, Nelson AR, Rege SV, Ramanathan A, Wang Y, Ahuja A, et al. Pericyte degeneration leads to neurovascular uncoupling and limits oxygen supply to brain. Nat Neurosci. 20:406–416.2017; [PubMed: 28135240]
18. Lawton MT, Rutledge WC, Kim H, Stapf C, Whitehead KJ, Li DY, et al. Brain arteriovenous malformations. Nat Rev Dis Primers. 1:15008.2015; [PubMed: 27188382]
19. Lebrin F, Srun S, Raymond K, Martin S, van den Brink S, Freitas C, et al. Thalidomide stimulates vessel maturation and reduces epistaxis in individuals with hereditary hemorrhagic telangiectasia. Nat Med. 16:420–428.2010; [PubMed: 20364125]
20. Li F, Lan Y, Wang Y, Wang J, Yang G, Meng F, et al. Endothelial Smad4 maintains cerebrovascular integrity by activating N-cadherin through cooperation with Notch. Dev Cell. 20:291–302.2011; [PubMed: 21397841]
21. Lindahl P, Johansson BR, Levéen P, Betsholtz C. Pericyte loss and microaneurysm formation in PDGF-B-deficient mice. Science. 277:242–245.1997; [PubMed: 9211853]
22. Mishra A, Reynolds JP, Chen Y, Gourine AV, Rusakov DA, Attwell D. Astrocytes mediate neurovascular signaling to capillary pericytes but not to arterioles. Nat Neurosci. 19:1619–1627.2016; [PubMed: 27775719]
23. Murphy PA, Kim TN, Huang L, Nielsen CM, Lawton MT, Adams RH, et al. Constitutively active Notch4 receptor elicits brain arteriovenous malformations through enlargement of capillary-like vessels. Proc Natl Acad Sci U S A. 111:18007–18012.2014; [PubMed: 25468970]
24. Pekmezci M, Nelson J, Su H, Hess C, Lawton MT, Sonmez M, et al. Morphometric characterization of brain arteriovenous malformations for clinical and radiological studies to identify silent intralesional microhemorrhages. Clin Neuropathol. 35:114–121.2016; [PubMed: 27049066]
25. Peppiatt CM, Howarth C, Mobbs P, Attwell D. Bidirectional control of CNS capillary diameter by pericytes. Nature. 443:700–704.2006; [PubMed: 17036005]
26. Rangel-Castilla L, Russin JJ, Martinez-Del-Campo E, Soriano-Baron H, Spetzler RF, Nakaji P. Molecular and cellular biology of cerebral arteriovenous malformations: a review of current concepts and future trends in treatment. Neurosurg Focus. 37(3):E1.2014;
27. Sagare AP, Bell RD, Zhao Z, Ma Q, Winkler EA, Ramanathan A, et al. Pericyte loss influences Alzheimer-like neurodegeneration in mice. Nat Commun. 4:2932.2013; [PubMed: 24336108]

28. Sato S, Kodama N, Sasaki T, Matsumoto M, Ishikawa T. Perinidal dilated capillary networks in cerebral arteriovenous malformations. Neurosurgery. 54:163–170.2004; [PubMed: 14683554]
29. Schulz GB, Wieland E, Wüstehube-Lausch J, Boulday G, Moll I, Tournier-Lasserve E, et al. Cerebral cavernous malformation-1 protein controls DLL4-Notch3 signaling between the endothelium and pericytes. Stroke. 46:1337–1343.2015; [PubMed: 25791711]
30. Sengillo JD, Winkler EA, Walker CT, Sullivan JS, Johnson M, Zlokovic BV. Deficiency in mural vascular cells coincides with blood-brain barrier disruption in Alzheimer's disease. Brain Pathol. 23:303–310.2013; [PubMed: 23126372]
31. Sweeney MD, Ayyadurai S, Zlokovic BV. Pericytes of the neurovascular unit: key functions and signaling pathways. Nat Neurosci. 19:771–783.2016; [PubMed: 27227366]
32. Thalgott J, Dos-Santos-Luis D, Lebrin F. Pericytes as targets in hereditary hemorrhagic telangiectasia. Front Genet. 6:37.2015; [PubMed: 25763012]
33. Tu J, Stoodley MA, Morgan MK, Storer KP. Ultrastructural characteristics of hemorrhagic, nonhemorrhagic, and recurrent cavernous malformations. J Neurosurg. 103:903–909.2005; [PubMed: 16304995]
34. Tu J, Stoodley MA, Morgan MK, Storer KP. Ultrastructure of perinidal capillaries in cerebral arteriovenous malformations. Neurosurgery. 58:961–970.2006; [PubMed: 16639333]
35. Winkler EA, Bell RD, Zlokovic BV. Central nervous system pericytes in health and disease. Nat Neurosci. 14:1398–1405.2011; [PubMed: 22030551]
36. Winkler EA, Bell RD, Zlokovic BV. Lack of Smad or Notch leads to a fatal game of brain pericyte hopscotch. Dev Cell. 20:279–280.2011; [PubMed: 21397835]
37. Winkler EA, Bell RD, Zlokovic BV. Pericyte-specific expression of PDGF beta receptor in mouse models with normal and deficient PDGF beta receptor signaling. Mol Neurodegener. 5:32.2010; [PubMed: 20738866]
38. Winkler EA, Sengillo JD, Bell RD, Wang J, Zlokovic BV. Blood-spinal cord barrier pericyte reductions contribute to increased capillary permeability. J Cereb Blood Flow Metab. 32:1841–1852.2012; [PubMed: 22850407]
39. Winkler EA, Sengillo JD, Sagare AP, Zhao Z, Ma Q, Zuniga E, et al. Blood-spinal cord barrier disruption contributes to early motor-neuron degeneration in ALS-model mice. Proc Natl Acad Sci U S A. 111:E1035–E1042.2014; [PubMed: 24591593]
40. Winkler EA, Sengillo JD, Sullivan JS, Henkel JS, Appel SH, Zlokovic BV. Blood-spinal cord barrier breakdown and pericyte reductions in amyotrophic lateral sclerosis. Acta Neuropathol. 125:111–120.2013; [PubMed: 22941226]
41. Yemisci M, Gursoy-Ozdemir Y, Vural A, Can A, Topalkara K, Dalkara T. Pericyte contraction induced by oxidativenitrative stress impairs capillary reflow despite successful opening of an occluded cerebral artery. Nat Med. 15:1031–1037.2009; [PubMed: 19718040]
42. Zeisel A, Muñoz-Manchado AB, Codeluppi S, Lönnerberg P, La Manno G, Juréus A, et al. Brain structure. Cell types in the mouse cortex and hippocampus revealed by single-cell RNA-seq. Science. 347:1138–1142.2015; [PubMed: 25700174]
43. Zhang R, Zhu W, Su H. Vascular integrity in the pathogenesis of brain arteriovenous malformation. Acta Neurochir Suppl. 121:29–35.2016; [PubMed: 26463919]
44. Zhao Z, Nelson AR, Betsholtz C, Zlokovic BV. Establishment and dysfunction of the blood-brain barrier. Cell. 163:1064–1078.2015; [PubMed: 26590417]

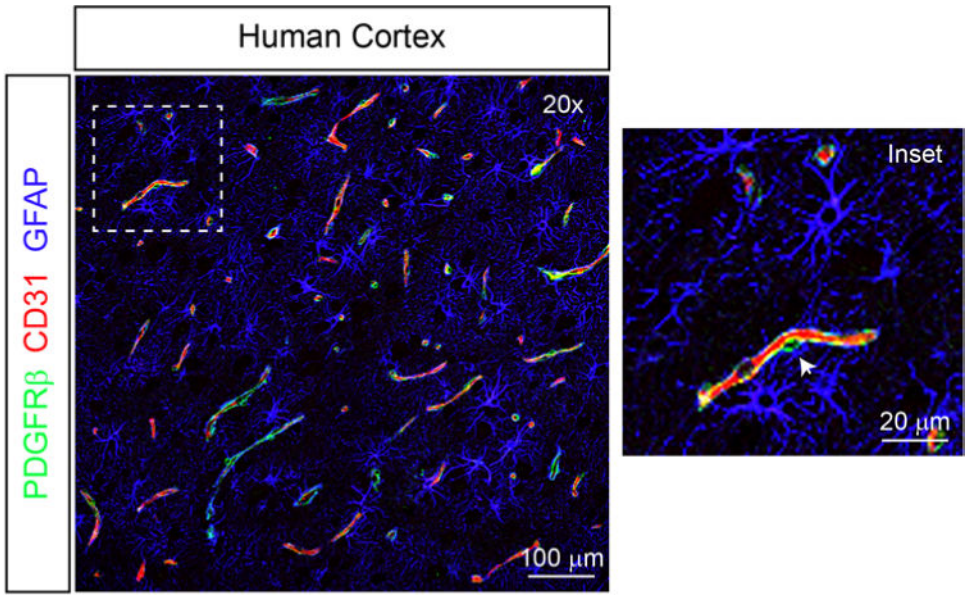

FIG. 1.

Cytoarchitecture of the cerebrovasculature in the human cortex. Representative low-magnification confocal microscopy image depicting the close structural relationship among pericytes (PDGFRβ, *green*), endothelial cells (CD31, *red*), and astrocytes (GFAP, *blue*) in human cortex. **Inset** features a higher-magnification view demonstrating a pericyte cell body (*arrowhead*) and contiguous stellate process, which ensheathe the endothelial wall.

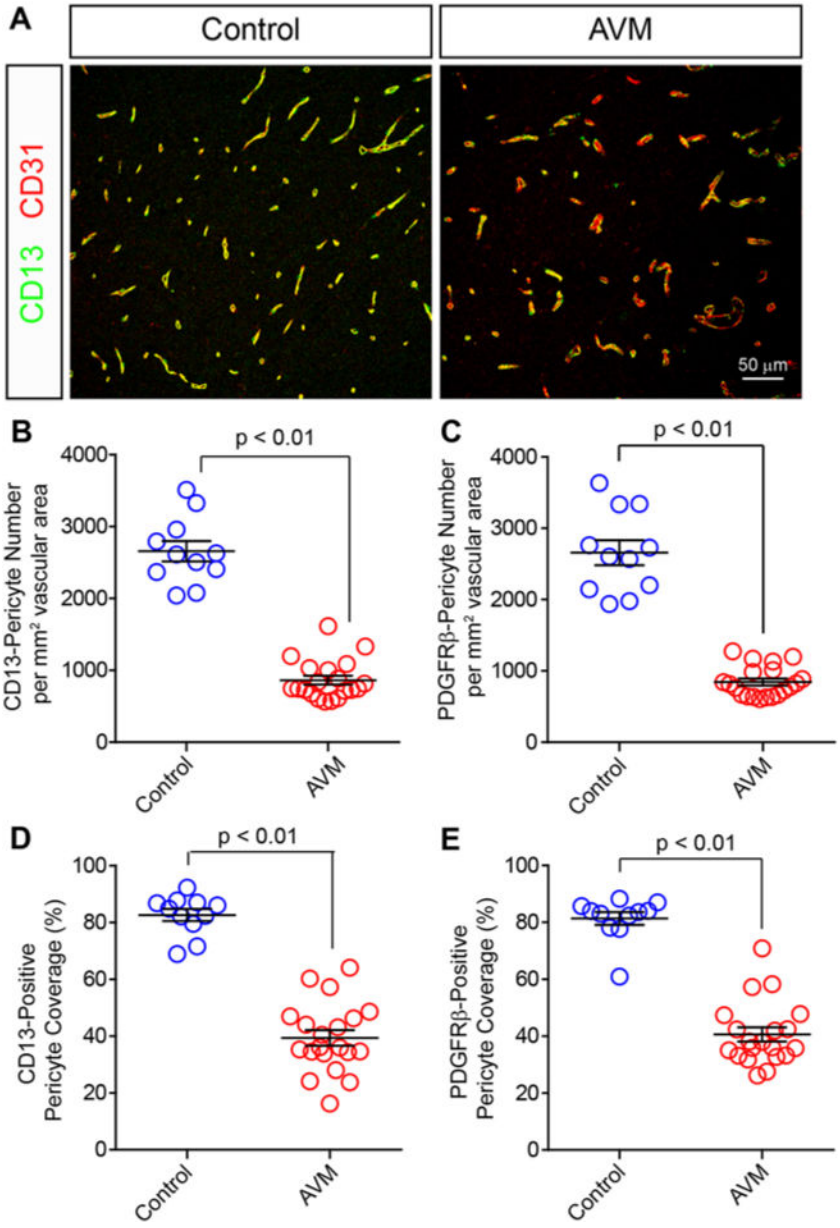

FIG. 2.

Vascular pericytes are reduced in human bAVMs. Representative confocal microscopy analysis (**A**) of CD13-positive pericytes (*green*) and CD31-positive endothelium (*red*) in human AVMs and temporal cortex from NVLCs. Graphs showing quantification of CD13-positive (**B**) and PDGFRβ-positive (**C**) pericyte cells per square millimeter vascular surface area in NVLCs and bAVMs. Graphs showing quantification of pericyte coverage of the vascular wall utilizing CD13 (**D**) and PDGFRβ (**E**) immunolabeling of pericyte cell processes. Values in the graphs are expressed as the mean ± standard error of the mean.

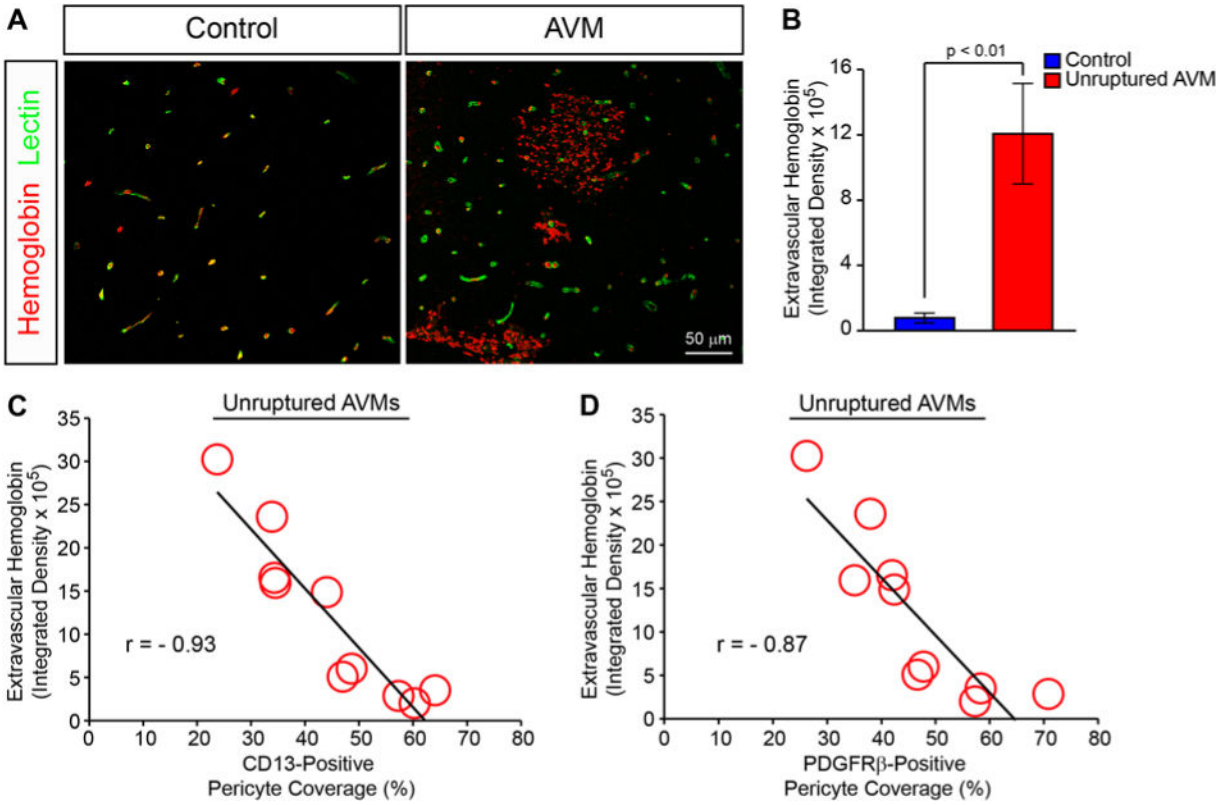

FIG. 3.

Reductions in vascular pericytes are associated with acute cerebral microhemorrhage in unruptured bAVMs. **A:** Representative confocal microscopy analysis of hemoglobin (*red*) and lectin-positive endothelium in temporal cortex from NVLCs and bAVMs. *Yellow* indicates colocalized intravascular hemoglobin. **B:** Graph demonstrating quantification of extravascular hemoglobin immunofluorescent signal from NVLCs (*blue*) and unruptured bAVMs (*red*). Values are expressed as the mean ± standard error of the mean. **C and D:** Graphic representation of correlation between CD13- or PDGFRβ-positive pericyte coverage and extravascular hemoglobin in unruptured bAVM tissue specimens.

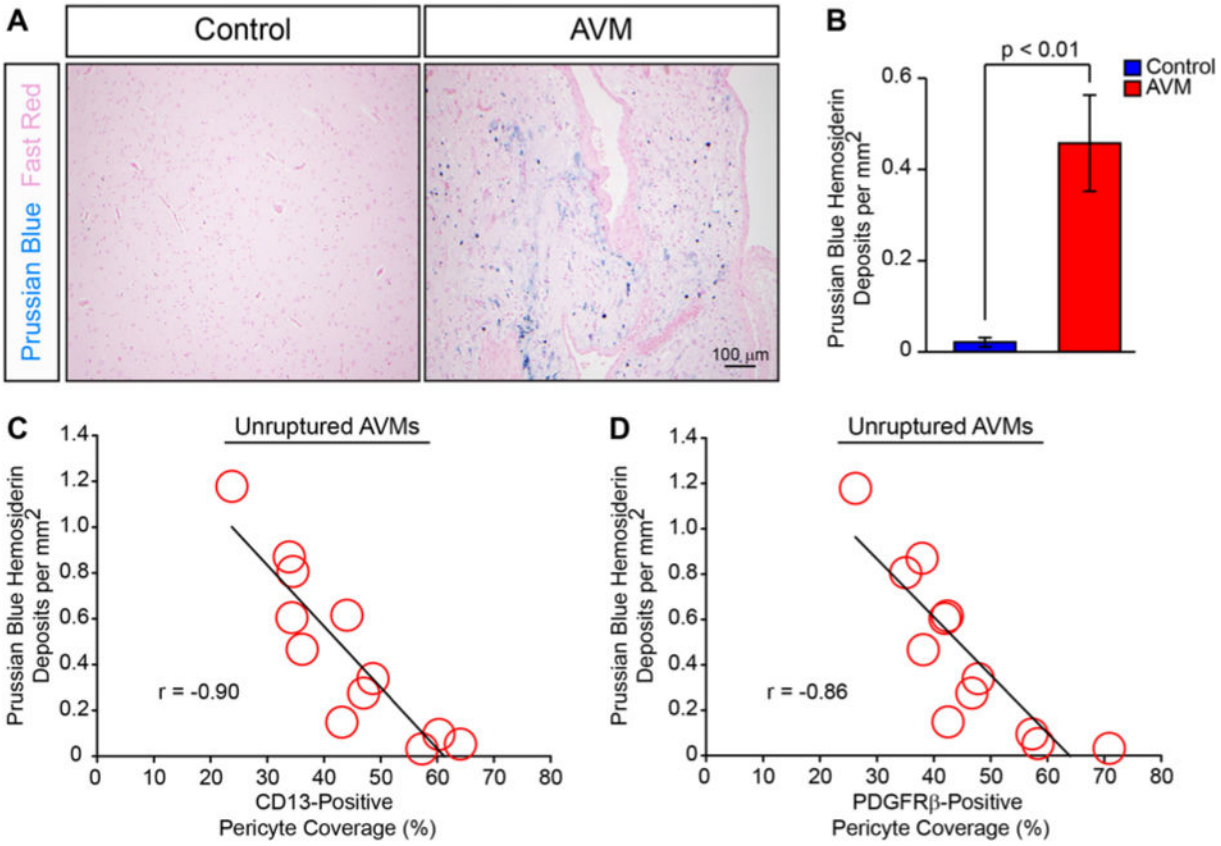

FIG. 4.

Pericyte reductions are associated and negatively correlated with chronic microhemorrhage in unruptured bAVMs. **A:** Representative bright-field microscopy analysis of Prussian blue–positive hemosiderin deposits (*blue*) with Nuclear fast red counterstain (*pink*) in bAVMs and temporal cortex from NVLCs. **B:** Graph demonstrating quantification of Prussian blue–positive hemosiderin deposits from NVLCs (*blue*) and unruptured bAVMs (*red*). Values are expressed as the mean ± standard error of the mean. **C and D:** Graphic representations of correlation between CD13- or PDGFRβ-positive pericyte coverage and hemosiderin deposition in unruptured bAVM tissue specimens.

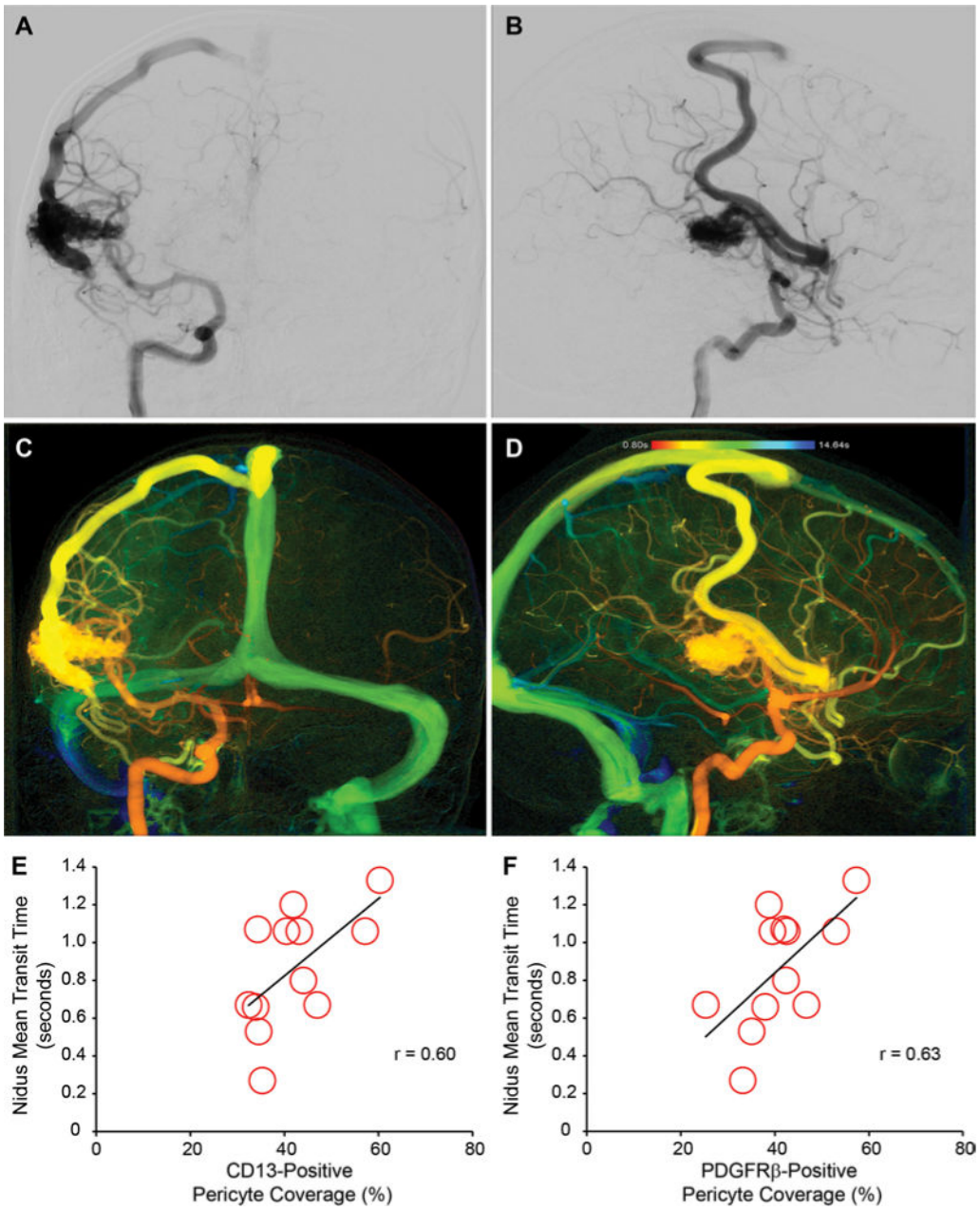

FIG. 5.

Pericyte reductions positively correlate with blood flow through the bAVM nidus. Representative preoperative angiograms, anteroposterior (**A**) and lateral (**B**) views of left internal carotid artery injection, demonstrating Spetzler-Martin grade II, supplementary grade 4 right lateral temporal bAVM. Representative syngo iFlow postprocessing of preintervention angiogram to determine mean iFlow transit time of bAVM nidus, anteroposterior (**C**) and lateral (**D**) views of left internal carotid artery injection. Graphic representations of correlation between CD13-positive (**E**) or PDGFRβ-positive (**F**) pericyte

coverage and MTT of blood flow through the bAVM nidus using iFlow analysis. Each point depicts an individual subject.

TABLE 1

Clinical characteristics of subjects providing tissue samples

Parameter	NVLCs	AVMs			p Value*
		Total	Unruptured	Ruptured	
No. of specimens	11	20	12	8	
Mean age in yrs	32.2 ± 7.0	33.2 ± 18.4	36.2 ± 16.0	28.6 ± 21.9	0.38
Sex	3 M/8 F	10 M/10 F	7 M/5 F	3 M/5 F	0.65
Lesion location					0.26
Supratentorial	11 (100)	16 (80)	11 (92)	5 (62.5)	
Infratentorial	0 (0)	4 (20)	1 (8)	3 (37.5)	
Lesion characteristics					
Nidus size	—	1.9 ± 0.8	2.2 ± 0.6	1.6 ± 1.1	0.12
Deep venous drainage	—	6 (30)	4 (33)	2 (25)	1.0
Eloquence	—	10 (50)	6 (50)	4 (50)	1.0
Spetzler-Martin grade					
Mean	—	2 ± 0.7	1.9 ± 0.7	2.1 ± 0.8	0.54
I	—	5 (25)	3 (25)	2 (25)	
II	—	10 (50)	7 (58)	3 (37.5)	
III	—	5 (25)	2 (17)	3 (37.5)	
IV	—	0 (0)	0 (0)	0 (0)	
V	—	0 (0)	0 (0)	0 (0)	
Supplemental grade†					
Mean	—	2.8 ± 1.1	3.3 ± 1.0	2.1 ± 0.8	0.01
1	—	2 (10)	0 (0)	2 (25)	
2	—	6 (30)	3 (25)	3 (37.5)	
3	—	6 (30)	3 (25)	3 (37.5)	
4	—	5 (25)	5 (42)	0 (0)	
5	—	1 (5)	1 (8)	0 (0)	
Presenting symptom					0.01

J Neurosurg. Author manuscript; available in PMC 2019 January 03.

Parameter	NVLCs	AVMs			p Value*
		Total	Unruptured	Ruptured	
Seizure	11 (100)	6 (30)	6 (50)	0 (0)	
Headache	—	9 (45)	5 (42)	4 (50)	
Altered mental status	—	4 (20)	0 (0)	4 (50)	
Incidental lesion	—	1 (5)	1 (8)	0 (0)	
Presurgical treatment					
Embolization	—	7 (35)	3 (15)	4 (50)	0.36
Radiosurgery	—	1 (5)	0 (0)	1 (8)	0.40

— = not applicable.

Values are expressed as the mean ± standard error of the mean or as number (%).

*Comparison between unruptured and ruptured AVMs.

†For additional information on the supplementary grading scale, see Lawton MT, Kim H, McCulloch CE, Mikhak B, Young WL: A supplementary grading scale for selecting patients with brain arteriovenous malformations for surgery. *Neurosurgery 66:*702–713, 2010.

J Neurosurg. Author manuscript; available in PMC 2019 January 03.

TABLE 2

Pericyte abundance and coverage values in NVLCs and bAVMs

Parameter	NVLCs	AVMs			p Value*
		Total	Unruptured	Ruptured	
Pericyte no.					
PDGFRβ-positive pericytes (per mm^2 endothelium)	2658.1 ± 174.8	845.6 ± 47.9†	844.9 ± 63.8	842.8 ± 77.4	0.99
CD13-positive pericytes (per mm^2 endothelium)	2657.0 ± 140.7	862.2 ± 61.4†	832.3 ± 71.7	907.1 ± 114.1	0.59
Pericyte coverage					
% PDGFRβ-positive pericyte coverage	81.3 ± 2.3	40.6 ± 2.5†	44.3 ± 3.6	35.1 ± 2.0	**0.04**
% CD13-positive pericyte coverage	82.7 ± 2.1	39.4 ± 2.8†	43.9 ± 3.2	32.6 ± 3.4	**0.03**

Boldface type indicates statistical significance.

*Unruptured compared with ruptured AVMs.

†All values statistically significant with $p < 0.01$ when NVLCs are compared with total AVMs.